Volume 58
Number 95
11 December 2022
Pages 13161–13288

ChemComm

Chemical Communications

rsc.li/chemcomm

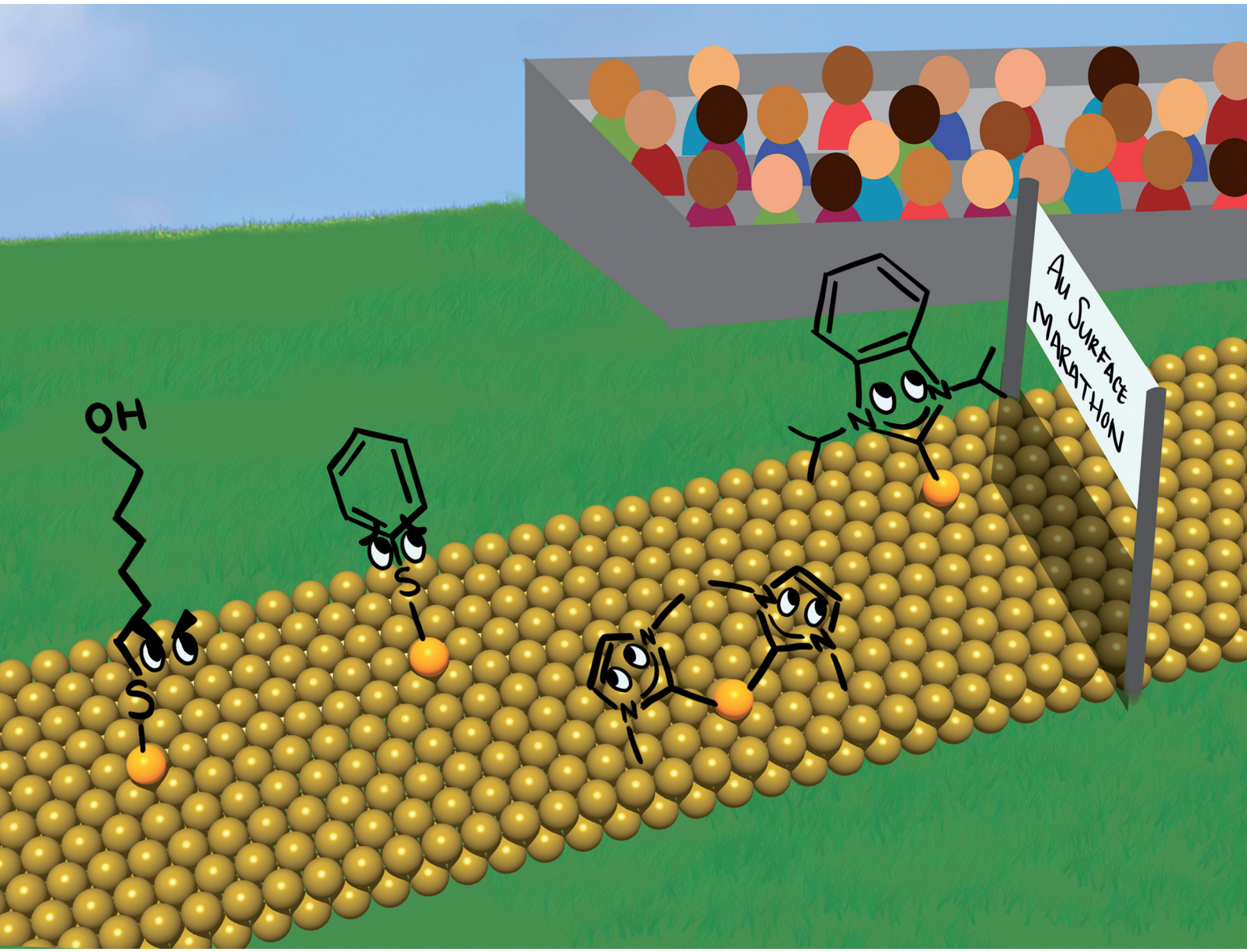

ISSN 1359-7345

ROYAL SOCIETY OF CHEMISTRY

FEATURE ARTICLE

Jon P. Camden, David M. Jenkins *et al.*

Fundamentals and applications of N-heterocyclic carbene functionalized gold surfaces and nanoparticles

ChemComm

ROYAL SOCIETY OF CHEMISTRY

FEATURE ARTICLE

View Article Online
View Journal | View Issue

Open Access Article. Published on 07 November 2022. Downloaded on 11/7/2025 11:57:10 PM.
This article is licensed under a Creative Commons Attribution-NonCommercial 3.0 Unported Licence.

Check for updates

Cite this: *Chem. Commun.*, 2022, **58**, 13188

Fundamentals and applications of N-heterocyclic carbene functionalized gold surfaces and nanoparticles

Gurkiran Kaur,[a] Rebekah L. Thimes,[b] Jon P. Camden *[b] and David M. Jenkins *[a]

Received 21st September 2022,
Accepted 1st November 2022

DOI: 10.1039/d2cc05183d

rsc.li/chemcomm

The discovery of N-heterocyclic carbenes (NHCs) revolutionized organometallic chemistry due to their strong metal–ligand bonds. These strong bonds also lend enhanced stability to gold surfaces and nanoparticles. This stability and high degree of synthetic tunability has allowed NHCs to supplant thiols as the ligand of choice when functionalizing gold surfaces. This review article summarizes the basic science and applications of NHCs on gold surfaces and gold nanoparticles. Additionally, scientific questions that are unique to gold–NHC systems are discussed, such as the NHC adatom binding motif and the NHC surface mobility. Finally, new applications for NHCs on gold are covered with particular attention to biomedicine, catalysis, and microelectronics.

Introduction

Gold surfaces and nanoparticles are responsible for applications ranging from medicine and sensing to catalysis and electronics.[1–6] In almost all cases, the functional properties of the gold arise from the molecules adsorbed to the noble-metal surface, not from the native gold substrate. Much of the success of these materials can be attributed to thiol-based self-assembled monolayers (SAMs) providing a tuneable and broadly applicable strategy for surface modification.[7–9] Despite widespread use, the shortcomings of thiols are numerous and well known. Extensive degradation of thiol-based surfaces has been observed in ambient conditions,[10–12] upon thermal treatment,[13–16] under UV exposure,[17–19] and in commonly-used biological media (Fig. 1A).[16,20–22] These limitations have led surface scientists to search for a more robust alternative for SAMs for gold surfaces and nanoparticles.

In organometallic chemistry, N-heterocyclic carbenes (NHCs) have been employed for complexation of gold due to their strong σ-bonds.[23,24] These gold complexes have found applications in catalysis,[25,26] potential cancer treatments,[23,27–30] and luminescence.[31–33] NHCs jumped from homogenous gold complexes to gold nanoparticles in two contemporaneous reports in 2009, one by Tilley and the other by Fairlamb and Chechik.[34,35] Then, just under ten years ago, multiple researchers in quick

[a] Department of Chemistry, University of Tennessee, Knoxville, Tennessee, 37996, USA. E-mail: jenkins@ion.chem.utk.edu
[b] Department of Chemistry and Biochemistry, University of Notre Dame, Notre Dame, Indiana, 46556, USA. E-mail: jon.camden@nd.edu

Gurkiran Kaur

Gurkiran Kaur received her BS and MS in Chemistry from Panjab University, Chandigarh, India. She then moved to the USA to pursue a PhD in Chemistry at the University of Tennessee under the supervision of Prof. David Jenkins. Her research focuses on the synthesis of N-heterocyclic carbenes (NHCs) for surface functionalization of gold surfaces and nanoparticles.

Rebekah L. Thimes

Rebekah L. Thimes received her BS in chemistry from Doane University, Crete, NE. She is currently pursuing her PhD in Chemistry at the University of Notre Dame under the supervision of Prof. Jon Camden. Her research focuses on the development of analyte detection schemes and the study of functionalized nanomaterials using surface-enhanced spectroscopies.

This journal is © The Royal Society of Chemistry 2022

Open Access Article. Published on 07 November 2022. Downloaded on 11/7/2025 11:57:10 PM.
This article is licensed under a Creative Commons Attribution-NonCommercial 3.0 Unported Licence.

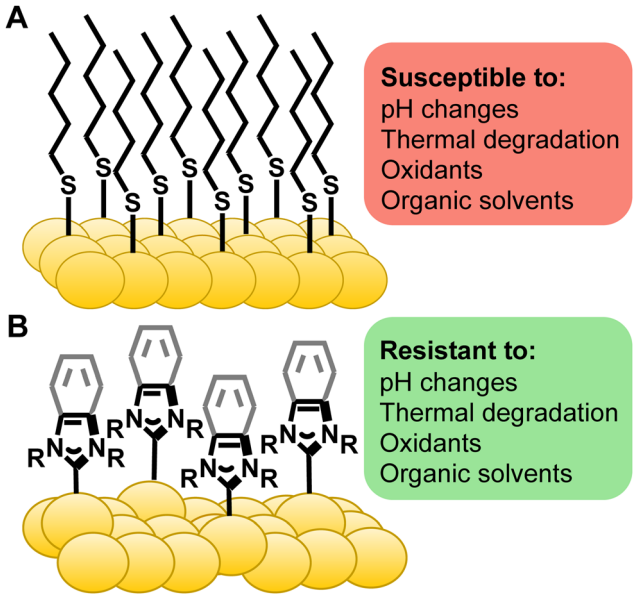

Fig. 1 Advantages of NHC SAMs over thiol SAMs on gold surfaces.

succession reported remarkable results of transferring NHCs to gold surfaces[36,37] and, critically, their impressive stability on gold. Crudden and Horton, in particular, noted that the NHCs are highly stable compared to thiols suggesting that these ligands could be the alternative ligand that surface scientists require (Fig. 1B).[38]

In this Feature Article, we will address both the key scientific findings and applications for NHCs on both gold surfaces and nanoparticles. We begin with a recap of the basic scientific questions: an assessment of the NHCs and gold surfaces that have been studied, a description of their synthesis and binding to the surface, and finally how researchers have evaluated these ligands on the surface. A separate section is devoted to reviewing applications. A similar format follows for NHCs on gold nanoparticles. Differences in NHCs' behaviour between gold surfaces and nanoparticles are noted throughout the manuscript. This review does not endeavour to be comprehensive, rather to summarize the key fundamental science questions surrounding NHC surfaces and highlight how NHCs can be a key driver for gold surface and nanoparticle technologies. The interested reader is also directed to other specialized[39–41] and comprehensive[42–45] reviews appearing recently.

Discussion

NHCs on gold surfaces

Classes of NHCs and gold surfaces investigated. Studies of NHCs on gold surfaces have focused primarily on the benzimidazolium and imidazolium classes of NHCs, which are often referred to as "standard carbenes". The synthesis, binding, mobility, stability, and characterization of these standard NHCs have been the subject of intense experimental and theoretical studies.[38,46–50] The R-groups attached to the NHC nitrogen, colloquially referred to as wingtips, strongly influence the NHC's binding and orientation to the surface, while R' groups attached to the backbone (facing away from the gold surface) modify the NHC's electronic structure and provide a modular binding site for molecular targets (Fig. 2). More recently, imidazolinium and cyclic (alkyl)(amino) carbene (CAAC) type NHCs were shown to bind gold surfaces, thereby expanding NHC surfaces to include non-standard carbenes.[48,51,52] Employing non-standard NHCs may improve stability on the surface due to improved σ-donor strength or increased π-backbonding.[53]

Turning to the surface, most previous work has focused on a limited selection of crystalline gold surfaces, with Au(111) being the most common.[47,54–56] Other crystalline gold surfaces such as Au(110) (2 × 1) have been employed to study the effect of surface reconstruction.[57] Amorphous gold mirrors and gold film-over nanospheres (AuFONs) surfaces have also been used to append NHCs for electrochemical or spectroscopic applications,[48,58,59] illustrating that crystalline surfaces are not required for robust NHC binding on gold.

Jon P. Camden

Jon P. Camden received his BS in chemistry and music from the University of Notre Dame and his PhD from Stanford University. Following postdoctoral work at Northwestern University, he joined the Department of Chemistry at the University of Tennessee before moving to the University of Notre Dame where he is currently a Professor in the Department of Chemistry and Biochemistry. His group's research interests range from the optical properties of nanoparticles and ultrasensitive detection methods to fundamental dynamics of simple chemical reactions.

David M. Jenkins

David M. Jenkins received his BA in chemistry from Cornell University and his PhD from the California Institute of Technology. After a Miller postdoctoral fellowship at UC Berkeley, he joined the Department of Chemistry at the University of Tennessee in 2008. In 2020, he became a Ziegler Professor of Chemistry and he also serves as Associate Head for the department. His group's research focuses on the design of novel azole ligands, including NHCs, for a wide variety of inorganic synthetic projects ranging from porous materials, to nanoparticles, to homogenous catalysis.

Open Access Article. Published on 07 November 2022. Downloaded on 11/7/2025 11:57:10 PM.
This article is licensed under a Creative Commons Attribution-NonCommercial 3.0 Unported Licence.

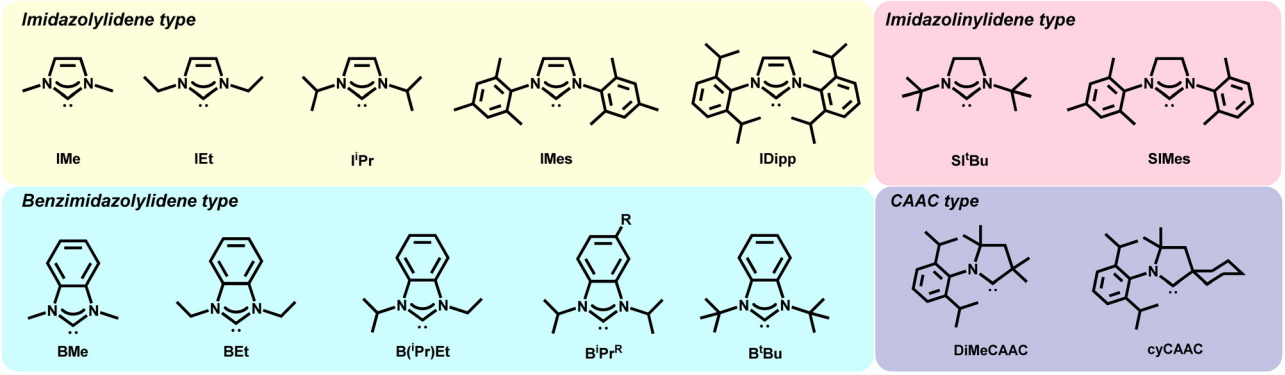

Fig. 2 Examples of NHCs that have been studied on gold surfaces and nanoparticles.

Synthesis of gold surfaces coated with NHCs. To date, Au–NHC self-assembled monolayers (SAMs) have been prepared by the four methods shown in Fig. 3. The first method (Fig. 3A) involves abstraction of a proton to generate the free carbene using strong bases, such as sodium or potassium *tert*-butoxide and potassium bis(trimethylsilyl)amide (KHMDS), in the presence of aprotic solvents like THF under an inert atmosphere.[37,38,56] There have been some reports where base residuals hinder the SAM formation, limiting which NHCs are applicable with this method.[60,61] These drawbacks can be circumvented by using either the imidazolium bicarbonate salts (Fig. 3B) or the NHC–CO_2 adducts (Fig. 3C) as precursors to generate free carbenes.[49,55,58,62–66] Heating these precursors under vacuum leads to evaporation (including loss of CO_2 + H_2O or CO_2, respectively) and deposition of the NHC on the gold surface. The synthesis of CO_2 adducts or bicarbonate salts, however, requires separation and ion exchange steps.[62] Furthermore, the incompatibility of protic functional groups with the hydrogen carbonate synthesis limits the use of these methods.[67] Finally, electrochemical deposition of NHCs onto gold surfaces under ambient conditions has recently been reported (Fig. 3D).[61] The reduction of water at negative potential results in the formation of hydroxide ions close to the electrode surface, leading to deprotonation of imidazolium.

Binding modes of NHCs onto gold surfaces. Understanding how NHCs bind to gold surfaces at the atomic level is perhaps one of the most fascinating scientific inquiries about NHCs on gold surfaces. The binding motifs of NHCs on gold surfaces are complex and different measurement techniques have focused on different aspects of this inquiry. Nevertheless, a clearer picture has emerged recently leading to a set of three binary questions to answer (Fig. 4). First, is the NHC bound directly to the flat gold surface or to a gold adatom? Second, is the NHC perpendicular to the surface or tilted? Finally, if the NHC is both tilted and on a gold adatom, are one or more NHCs bound to the same adatom? These disparate binding motifs to gold surfaces have been explored theoretically using DFT calculations[47] and experimentally using high-resolution electron energy loss spectroscopy (HREELs) and high-resolution electron microscopy.

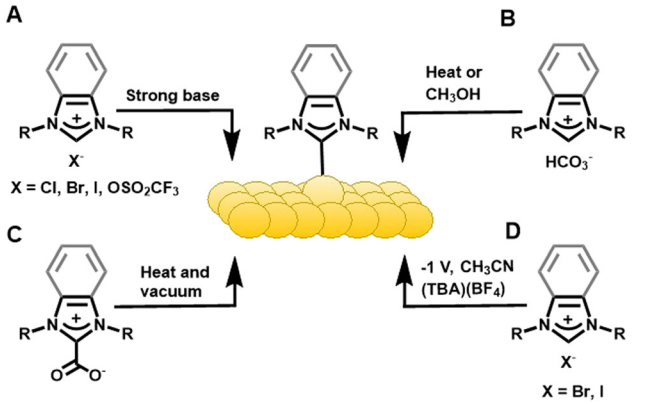

Fig. 3 Methods employed for deposition of NHCs on gold surfaces.

The distinct binding motifs observed can be attributed to both the class of NHC employed as well as the substituents off the nitrogen atoms (wingtips). Imidazole NHCs with small wingtips, such as methyl, lie flat on the surface and can also adopt the dimer configuration (Fig. 4C).[55] Conversely, imidazole NHCs with relatively bulky isopropyl (I^{i}Pr) and diisopropylphenyl (IDipp) groups are oriented perpendicular to the surface on an adatom as shown in Fig. 4B, left.[50,55]

NHCs with longer straight chain wingtips give rise to more complicated interactions with the gold surface. Butyl wingtips increase the van der Waals interactions with the surface and, hence, favors a tilted motif. In addition, dimeric complexes for these NHCs have been observed upon annealing with the two NHCs connected by a gold adatom (Fig. 4C, right).[50]

In a similar fashion, different binding modes have been observed for benzimidazolium-based NHCs. Small wingtips on BMe and BEt (Fig. 2) align parallel to the surface on an adatom as shown in Fig. 4B, right.[46] The B^{i}Pr NHC has been studied extensively due to formation of stable monolayers and easy deposition, but its binding motif is anything but simple. B^{i}Pr can align either in a tilted fashion at a 40° angle (Fig. 4B, right)[55] or stand upright on the surface (Fig. 4B, left).[46,54] Furthermore, dimeric B^{i}Pr–Au–B^{i}Pr species (Fig. 4C, right) can be observed when the surface coverage of the NHC is low.[54,55] In contrast, the bulkiest wingtips, *tert*-butyl, on B^{t}Bu leads to upright binding exclusively on an adatom (Fig. 4B, left).[54]

Open Access Article. Published on 07 November 2022. Downloaded on 11/7/2025 11:57:10 PM.
This article is licensed under a Creative Commons Attribution-NonCommercial 3.0 Unported Licence.

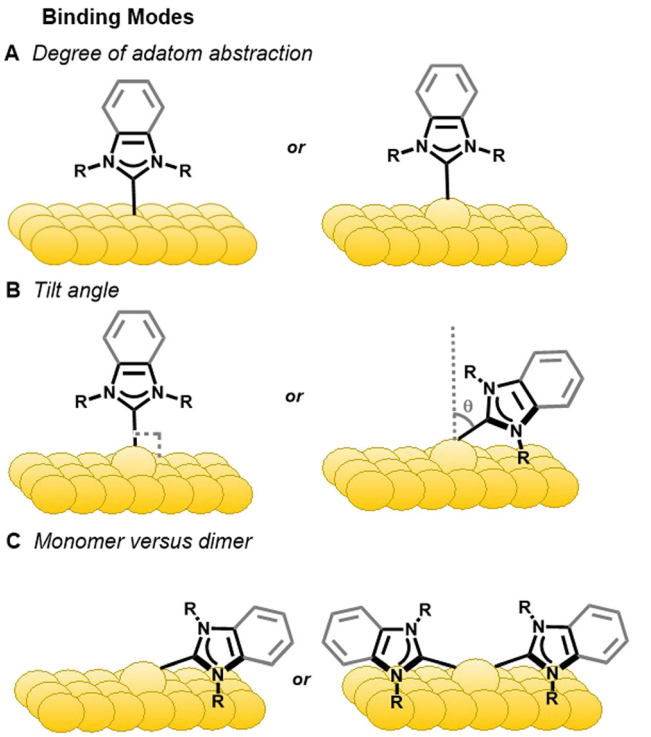

Fig. 4 Schematic of different considerations for binding of NHCs to gold surfaces. (A) Depicts level of abstraction of gold atom from surface leading to an adatom. (B) Depicts vertical *versus* tilted NHCs on surfaces. (C) Depicts monomer *versus* dimer formation for NHCs that are in a tipped configuration on surfaces.

Very recently, Glorius, Fuchs, and Du employed cyclohexyl CAAC (cyCAAC) on NHCs to study their binding and achieve reversible switching on Au(111).[51] The 6-membered aliphatic cyclohexyl side group was believed to rotate between two positions and is responsible for conformational switching of NHCs on the gold lattice.

Mobility of NHCs on gold surfaces. Since NHCs most commonly bind to adatoms on gold surfaces during the formation of a SAM, they are potentially mobile on the surface. Fuchs and Glorius investigated IDipp, IMes, and IMe (Fig. 2) *via* scanning tunneling microscopy (STM) to track this mobility on Au(111).[63] The IDipp and IMes both bind to the gold surface perpendicular to the surface on an adatom (Fig. 4B, left). In case of IDipp, islands of ligands were observed upon increased coverage of the monolayer. STM images clearly depicted the breaking and recombining of these islands on the surface. This motion was attributed to the binding of NHC to an adatom, which could then travel as a ballbot on the surface (Fig. 5). In contrast, STM images of IMes on Au(111) showed ellipsoidal shaped structures confirming no molecular rotation on the surface and no mobility. Owing to the less hindered side groups, IMe shows high mobility and aggregates to form dimeric and trimeric NHC complexes (Fig. 4C, right), which complicates the study of its mobility *versus* IDipp. Finally, Amirjalayer confirmed the generality of ballbot motion of adatoms on an Au(110) (2 × 1) surface.[57] The ballbots coordinate *via* a push–pull mechanism to reconstruct the gold surface.

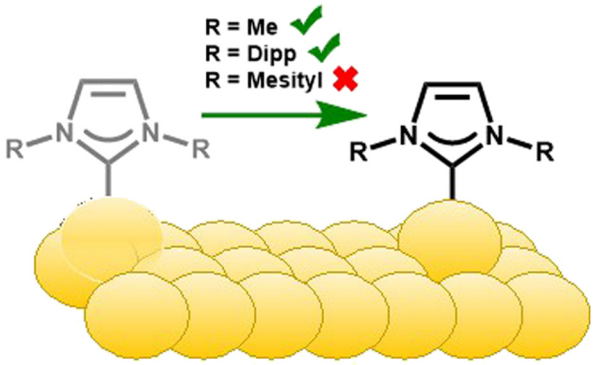

Fig. 5 Schematic depicting mobility of NHCs on gold surfaces. Some NHCs move with a ballbot motion, but others are tethered in place based on the wingtips employed.

NHCs' stability on gold surfaces. One important factor driving the rapid research on Au–NHC surfaces is their excellent thermal and chemical stability, particularly when compared to analogous Au-thiol SAMs. The majority of stability tests have been conducted on isopropyl winged NHCs (Fig. 2). SAMs of B^{i}Pr showed no degradation upon heating in water, THF, or decalin for 24 hours demonstrating thermal stability in multiple solvents.[38] SAMs of B^{i}Pr are resistant to oxidation when treated with 1% H_2O_2 and can withstand extreme pH conditions.[38,58] NHCs with aryl wingtips like IMes were also tested for stability, but due to less dense packing and relatively poor ordering, these IMes NHC SAMs are comparatively less stable than B^{i}Pr.[38] B^{i}Pr modified at the 5' position was also found to be quite stable upon ultrasonic treatment in water.[68] Even smaller NHCs, such as BMe, form SAMs with excellent thermal stability.[69] Recently, Camden and Jenkins compared the stability of different classes of NHCs and found that SAMs of SI^{t}Bu showed no degradation when exposed to 1 M HCl over 24 hours whereas I^{i}Pr SAMs decomposed under similar conditions.[48]

Characterization of NHCs on gold surfaces. Multiple experimental techniques have been employed to determine the binding modes, surface geometry, and stability of NHCs on gold including: STM, X-ray photoelectron spectroscopy (XPS), HREELS, and surface enhanced Raman spectroscopy (SERS). Microscopy methods have dominated studies on NHC surface binding while spectroscopic techniques have proven effective for monitoring stability of the NHC SAMs under atmospheric conditions. These techniques are often combined with theoretical calculations to provide a more detailed understanding of each system.

STM can observe ordered monolayers of NHCs on gold surfaces,[54,57,62] binding modes of NHCs with different wingtip groups,[46,50] surface mobility of NHCs on adatoms,[63] and temperature dependence of NHC SAMs.[54] Most of the binding studies of NHCs have been carried out by STM measurements.

XPS along with near edge X-ray absorption fine-structure spectroscopy (NEXAFS) have also been used in conjunction with DFT to predict NHC bonding and geometry.[55,56] NEXAFS has

Open Access Article. Published on 07 November 2022. Downloaded on 11/7/2025 11:57:10 PM.
This article is licensed under a Creative Commons Attribution-NonCommercial 3.0 Unported Licence.

been applied to determine the orientation of NHCs (Fig. 4). The NEXAFS intensity at near 401 eV corresponds to 1s → π* LUMO transition that originates on a nitrogen atom.[55] The intensity of this peak depends upon polarization of photons and varies with the substituents attached to the nitrogen.

Two surface spectroscopies, HREELS and SERS, when combined with DFT, have provided evidence of the binding mode of NHCs on the surface as well as the orientation of the wingtips. HREELS has been employed to predict tilted *versus* upright binding for BMe *versus* B^{i}Pr.[46] SERS has been employed to characterize NHC SAMs. Jenkins and Camden used NHCs with orthogonal functionalities as SERS tags to observe vibrations in the silent region.[58] Isotope labeling of NHCs with deuterium was combined with SERS measurements and coupled with DFT to determine whether I^{i}Pr and B^{i}Pr bound vertically on an adatom.[49]

Applications of NHC coated gold surfaces. The promise of improved NHC stability relative to thiols (Fig. 1) has prompted investigators to test their potential across a wide range of applications. NHC SAMs on gold surfaces have been explored for applications ranging from biomedical research to microprinting to electronics. Not only have the NHCs improved the stability of the devices, but in some cases, additional benefits over commercially available thiol counterparts were noted.

Label-free sensing[70] of biochemical analytes is of critical importance for developing medical diagnostics.[71,72] Crudden and Horton adapted surface plasmon resonance (SPR) biosensors to use NHCs on gold. Carboxymethylated dextran and streptavidin (SA) were the bioactive linkers that then detected biotin.[62] Diisopropyl-benzimidazolium hydrogen carbonate, a bench stable NHC precursor, was used to form chemically and electrochemically stable NHC films on Au(111) *via* methanol solution or vacuum deposition (Fig. 3C). The NHC-coated gold chips outperformed the commercially available thiol-derived hydrophobic association chips (HPA) in temperature and pH swing tests. This hydrophobic association-based biosensor was then used to detect lipid-binding analytes and was consistent with results from commercial SA chips. Horton expanded on this idea and paved the way for designing versatile NHC-based biosensor surfaces to widen the scope of this application.[73] The alkylated NHC SAM showed improved thermal and chemical stability, faster equilibration time, and greater shelf life than its thiol counterpart. Hao and Horton developed an NHC-based carboxymethylated dextran chip (NHC-CM) and then compared it to commercially available thiol-based CM5 and CM3 chips.[74] Surface analysis results of the NHC-CM showed high thermal stability, resistance to the non-specific adsorption of proteins, and improved homogeneity *versus* thiol SAMs. The performance of the NHC biosensor surface was validated with drug–plasma protein and antibody–antigen binding tests. The SPR performance of NHC-CM chips was comparable with the commercial chips in kinetic analysis. Later, Horton used dextran NHC SAMs modified with SA, nitrilotriacetic acid (NTA), or recombinant Protein A, to sense biotin, histidine-tagged molecules, or antibodies, respectively.[59] NHC-SA chips showed biotinylated HetR-specific DNA interaction and the results were comparable to commercial SA-functionalized CM3 chips.

Rapid and accurate detection of pathogens is critically important for public health,[75] so Birss and Crudden developed an antibody-based electrochemical biosensor to detect the measles virus in minutes.[76] Their gold electrode was modified with an ethyl ester functionalized benzimidazolium trifluoromethanesulfonate. The NHC coated electrode produced a 10× larger response than an electrode coated with 6-mercaptohexanoic acid. A similar strategy was employed for electrochemical detection of bacteria.[77] Electrodes with NHC SAMs immobilized multiple toll-like receptor (TLR) proteins. The robustness of these TLR biosensors was tested by monitoring electrochemical-impedance spectroscopy (EIS) to sense bacteria from lake water. The sensor was extremely stable over a range of electrochemical voltages and could detect pathogens even after storing for four weeks.

Since the Au–C bond of an NHC may exhibit higher conductivity than an Au–S bond of a thiol,[78,79] molecular electronics applications could benefit from NHC SAMs on gold. Ravoo and Glorius communicated the first example of NHCs on gold for micro-contact printing (μCP), a soft-lithography technique.[65] Bench stable NHC–CO_2 adducts of BMe were used as NHC precursors owing to their compatibility with polar protic solvents and elastomeric stamps. Successful patterns of azide-terminated NHCs were observed on gold at 55 °C and these decorated areas showed higher conductivity. The undecorated region was then filled with a second, distinct, NHC with azide on *N*-substituted side chain. This functionalization paved the way for copper-catalyzed azide–alkyne cycloaddition with mannose and biotin. She, Kraatz, and Crudden extended this μCP application in a subsequent report.[80] In this case, the gold surface was decorated by sequentially depositing thiols and NHCs. Copper reduction using chronoamperometry was carried out to deposit copper (on the NHC area) that led to the formation of a metallic copper grid, which could subsequently be lifted off from the electrode and transferred. Venkataraman and Roy measured electron transfer properties across NHC–metal interfaces (Au, Ag, and Cu) in single-molecule junctions.[81] An exponential decay in conductance was observed upon extension of the backbone of the NHC ligand in the junction. Finally, Chi, Glorius, Wang, and Doltnis reported gold surfaces modified with NHCs for organic field-effect transistors (OFETs).[79,82] Transistors modified with 5 mmol IDipp NHCs showed greater stability, increased hole mobility, and reduced contact resistance at the gold-pentacene interface *versus* similarly processed transistors with 4-(trifluoro-methyl) benzenethiol.[79]

Photoswitches are a critical component for applications as diverse as conducting polymers to OLEDs,[83] and they often take advantage of *cis*/*trans* isomerism in azobenzene. Glorius and Ravoo built the first NHC-based molecular photoswitch by connecting arylazopyrazole (AAP) to an NHC.[83] After attaching the modified NHC to gold, the AAP moiety was oscillated from *cis* to *trans* through alternating UV and green light.

NHCs on gold nanoparticles

Classes of NHCs and gold nanoparticles investigated. AuNPs are valuable nanostructures due to the ease of tuning their size

 This journal is © The Royal Society of Chemistry 2022

Open Access Article. Published on 07 November 2022. Downloaded on 11/7/2025 11:57:10 PM.
This article is licensed under a Creative Commons Attribution-NonCommercial 3.0 Unported Licence.

and shape, their high biocompatibility, and their optical properties.[84,85] NHCs have been appended to spherical AuNPs ranging from non-plasmonically active NPs with a diameter of 1–2 nm to plasmonically active NPs with a diameter of >20 nm.[86] While most colloidal investigations of NHCs have been limited to spherical NPs, Johnson and co-workers reported functionalization of NHCs on CTAB-stabilized gold nanorods (AuNRs).[87]

As with gold surfaces, the exact organic moieties on the NHCs matter for gold nanoparticles. Modifications made at the wingtips can influence NHC stability and NP binding (Fig. 6), while modifications at the backbone positions create a handle for post-synthetic modification reactions (Fig. 6).[53,67] For example, the synthesis of water soluble NHCs through functionalization of the backbone or wingtip groups with hydrophilic polymeric chains or charged functional groups can improve biocompatibility.[88,89] Likewise, the synthesis of chiral NHCs is important for applications in asymmetric catalysis and chiral biomolecule discrimination.[90,91]

Synthesis of AuNPs with NHCs. There are two complementary approaches for synthesizing NHC–AuNPs: a bottom-up approach involving the direct reduction of an NHC gold complex and a top-down approach involving an NHC ligand migration to preformed AuNPs (Fig. 7).[34,35] The size of NHC–AuNPs synthesized *via* the bottom-up approach is highly dependent on the reaction conditions. Strong reducing agents like $NaBH_4$ yield smaller NPs (~1–4 nm),[90] while more mild reducing agents like $^tBuNH_2{\cdot}BH_3$ yield slightly larger NPs (~5–6 nm) with a wider size dispersion.[92]

NHCs can be transferred to the AuNPs in a top-down approach as free carbenes,[93,94] CO_2 adducts[95] or related bicarbonate salts,[95] and gold complexes.[67] Camden and Jenkins reported a general method for the transfer of NHC–Au(I) complexes to AuNPs in the first top-down synthesis yielding NPs

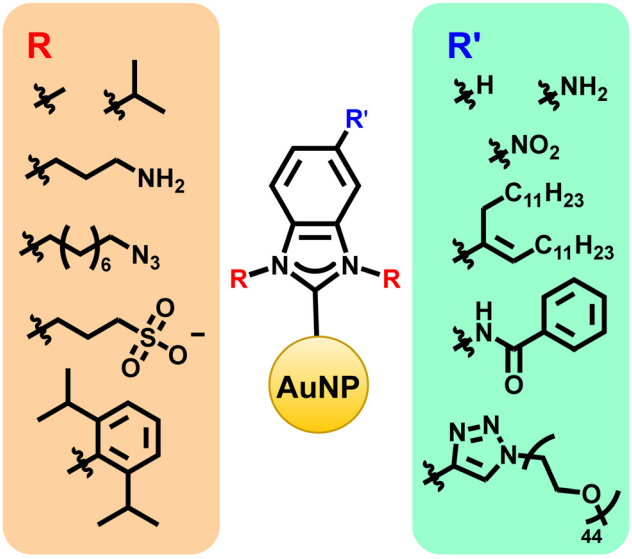

Fig. 6 Selected backbone and wingtip groups for benzimidazolium NHCs on gold nanoparticles.

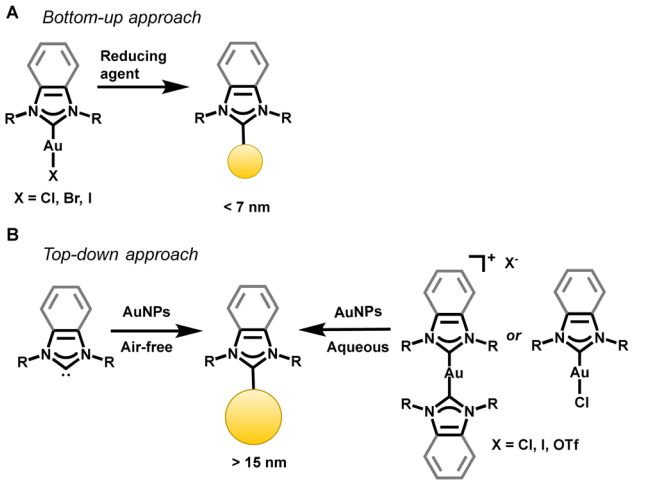

Fig. 7 Synthetic approaches to append NHCs to AuNPs. Both bottom-up and top-down approaches have proven successful.

with a diameter greater than 15 nm.[67] The top-down synthesis involving an NHC–Au complex has been hypothesized to lead to the addition of an adatom on the surface, rather than the extraction of an existing atom from the underlying gold lattice.[87] Johnson demonstrated improved stability of top-down synthesized NHC–AuNPs through an adatom addition, eliminating the need for gold lattice reorganization normally seen with the addition of NHCs to AuNPs.[87]

NHC capped AuNPs' stability. The practical applications of NHC–AuNPs require stability in thermal, chemical, and biological conditions. Many factors can impact the stability of the NHC–AuNPs including the synthetic method used, the denticity of the NHC ligand, NHC wingtip, AuNP size, and density of NHCs on the surface. The stability of NHC–AuNPs is characterized by two main criteria: (1) resistance to NP aggregation or change in morphology and (2) retention of the NHC–Au bond on the nanoparticle.[41]

AuNPs coated with NHCs generally have excellent thermal stability. Crudden functionalized 3 nm AuNPs with a series of mono and bidentate benzimidazolium NHCs that exhibited high stability when heated at 130 °C for 24 hours.[93] TEM images of the particles before and after thermal treatment displayed a slight increase (~1 nm) in particle diameter for the bidentate systems, and a larger increase (~2.3 nm) in diameter for the monodentate systems. Lissel and Fery also found that increasing the denticity of their poly(3-hexylthiophene)-NHCs resulted in NHC–AuNPs with increased thermal stability when heated for 24 hours at 100 °C.[96] As expected, multidentate NHC systems provide greater thermal stability to AuNPs against particle ripening.

The chemical stability of NHCs on AuNPs has been tested under both acidic and basic conditions. Crudden synthesized 2–3 nm water soluble benzimidazolium NHC–AuNPs with a carboxylate modified backbone that are soluble in organic solvents when protonated.[97] These NPs were found to be stable for 1–2 months in basic conditions, but displayed a reversible pH dependent aggregation when put in acidic conditions.

Open Access Article. Published on 07 November 2022. Downloaded on 11/7/2025 11:57:10 PM.
This article is licensed under a Creative Commons Attribution-NonCommercial 3.0 Unported Licence.

Reithofer synthesized ∼4.2–4.5 nm water-soluble imidazolium NHC–AuNPs containing a backbone substituted carboxylic acid that were stable in ambient conditions for at least 72 days, 150 mM NaCl for 14 days, and also showed reversible pH dependent aggregation.[98] Nazemi's polymeric mesoionic NHC–AuNPs were stable under basic (pH 12) as well as acidic (pH 2) conditions for 10 days with no significant change in their NP size or shape.[99] As an extreme test of chemical stability, Johnson exposed bidentate NHC-thiolate protected gold nanorods to gold etching conditions, and these NHC–gold nanorods showed complete resistance to 50 mM KCN for up to ten minutes.[87]

For NHC–AuNPs to be implemented in biomedical applications, they must be water-soluble and demonstrate stability in biological media. Johnson and MacLeod functionalized the AuNPs with PEGylated NHC ligands and reported water-soluble AuNPs. These NHCs displayed stability over a wide range of pH (3–14) for 24 hours, in various buffers for seven weeks, in cell culture media, and fetal bovine serum (FBS) for 26 hours.[100] Mattoussi functionalized ∼9 nm AuNPs with multidentate imidazolium NHCs modified with poly(ethylene glycol) chains that were stable for greater than one year in phosphate buffered saline (PBS) buffer over a wide pH range (pH 3–12).[94] Nazemi synthesized polymerized mesoionic NHC–AuNPs through a bottom-up approach that displayed high stability in fetal bovine serum (FBS) for two days.[99] Casini synthesized mono and bidentate imidazolium NHCs with sulfonate wingtip groups to achieve 2–5 nm water soluble AuNPs that displayed high stability in bovine serum albumin (BSA) for 48 hours.[101] Camden and Jenkins explored the stability of 19 nm AuNPs functionalized with imidazolium NHC ligands with isopropyl wingtips in different buffer solutions (PBS, tris-glycine potassium, tris-glycine potassium magnesium), cell culture media, and full strength human serum.[102] The NHC–AuNPs displayed high stability in all biological media for at least 21 days, with no significant changes observed in the SERS or XPS spectra due to changes in the NHC ligands on the surface.

Another challenge in expanding NHC–AuNPs for biological applications is their stability in the presence of biologically relevant thiols. Exogenous thiols can degrade both thiol and NHC-functionalized AuNPs through displacement of the surface ligands.[103] Increasing the denticity of the NHC ligands[87,93] or self-assembly of amphiphilic NHC–AuNPs in polar solvents[103] leads to higher resistance *versus* thiol-induced degradation. Nazemi polymerized mesoionic NHC–AuNPs that exhibited superior stability when exposed to 6 mM glutathione (GSH) for seven days.[99] However, when tested at a biologically relevant temperature of 37 °C, the AuNPs stability was limited to only 24 hours. Nazemi also developed a fluorescence scheme to quantify the amount of NHC ligands that desorb from their water-soluble NHC–AuNPs in the presence of GSH, finding that ∼45% of NHCs were displaced within one week of exposure to 4 mM GSH.[88]

Characterization of NHC capped AuNPs. Measurement of the size and shape of NHC–AuNPs as well as tests of their stability against aggregation or sintering is most often assessed by UV-vis, TEM/SEM, polyacrylamide gel electrophoresis (PAGE), dynamic light scattering (DLS), and inductively coupled plasma mass spectrometry (ICP-MS). The localized surface plasmon resonance (LSPR) peak in a UV-vis spectrum is indicative of the size, shape and aggregation state of the AuNPs.[104] The LSPR peak for small (∼3 nm) AuNPs usually appears around 520 nm and will red shift with increasing NP size, while the complete loss of the LSPR peak is usually attributed to aggregation of the AuNPs.[89] TEM/SEM images are used to discern the size and shape of nanoparticles and observe morphological changes after surface modifications or exposure to chemical and biological conditions.[103] PAGE provides insight into AuNP size and dispersity through size-dependent species separation in a gel matrix.[89] DLS measurements give an approximation for the hydrodynamic radius of the AuNP solution and are often coupled with zeta potential measurements which report the surface charge.[102] ICP-MS has also been used to characterize the stability of NHC–AuNPs by quantifying the amount of dissolved ionic gold.[105]

The formation and dissociation of the NHC–Au bond has been investigated using molecular or surface specific techniques like X-ray photoelectron spectroscopy (XPS), ^{1}H NMR and ^{13}C NMR, Fourier-transform infrared attenuated total reflectance (FTIR-ATR) spectroscopy, electrochemistry, and matrix assisted laser desorption ionization mass spectrometry (MALDI-MS). XPS is a technique for examining the elemental composition of a surface, in which the presence or absence of molecular species on the surface can be determined by looking in specific regions of the XPS spectra.[106] This technique was used to determine if any NHC was displaced or if dodecanethiol was incorporated into the monolayer by looking at the N (1s) and S (2p) regions of the XPS spectrum, respectively.[93] ^{1}H NMR and ^{13}C NMR are used to verify the binding of NHCs on AuNPs through the disappearance of the imidazolium proton and the down-field shift of the coordinating carbon peak, respectively.[90,94] FTIR-ATR is also often used to observe the absence of the imidazolium proton upon binding to the AuNP surface.[101] The extent of functionalization on the AuNP surface can be determined through electrochemical measurements. He and Liu evaluated the electrochemically active surface area (ECSA) of their NHC–AuNPs using cyclic voltammetry.[95] A decrease in the ECSA leads to a reduction in the surface oxygen monolayer, which was attributed to the presence of NHC ligands on the AuNP. MALDI-MS has been employed to observe NHC functionalized gold clusters that are ejected from ultrasmall AuNPs.[107]

Chemical reactions on the surface of AuNPs after deposition of the NHCs can also be tracked. These post-synthetic modifications of NHC–AuNPs have been explored by Camden and Jenkins using SERS[67] and laser desorption ionization mass spectrometry (LDI-MS).[108] A nitro-functionalized NHC–Au(I) complex was appended to AuNPs and reduced *in situ* to yield amine-functionalized NHC–AuNPs followed by an *in situ* amide coupling with benzoic acid.

Applications of NHC capped AuNPs. AuNPs are widely used in catalysis as their activity and selectivity can be tuned by modifying the shape, size, support structure, and stabilizing

 This journal is © The Royal Society of Chemistry 2022

Open Access Article. Published on 07 November 2022. Downloaded on 11/7/2025 11:57:10 PM.
This article is licensed under a Creative Commons Attribution-NonCommercial 3.0 Unported Licence.

ligand of the AuNPs.[109] NHC–AuNPs have been used in the lactonization of allene-carboxylic acids,[91] hydration and hydroamination of alkynes,[110,111] electroreduction of CO_2,[95] and hydrogenation of nitroarenes.[112] Finally, Casini utilized water soluble mono and bidentate NHC ligand-stabilized AuNPs for the catalytic reduction of nitrophenols and resazurin.[101]

AuNPs have also displayed great potential in the field of biomedicine as a platform for photomediated processes, such as photothermal therapy (PTT) and photoacoustic (PA) imaging, due to their ability to efficiently convert absorbed light into thermal energy.[113] The *in vitro* PTT capabilities of NHC–AuNPs were first investigated in 2018 by Johnson through the use of bidentate thiolate-imidazolium stabilized gold nanorods to induce MCF7 human breast adenocarcinoma cell death.[87] The NHC–gold nanorods showed high cell viability prior to laser irradiation, but led to significant cell killing upon exposure to near-IR (NIR) radiation for several minutes. Casini also evaluated the PTT capabilities of their bidentate NHC–AuNPs through *in vitro* studies with human PC-3 prostate cancer cells.[101] Their NHC–AuNPs displayed modest photothermal efficiency, but notably gold nanorods have been shown to be a more efficient structure for photothermal heating than spherical nanoparticles.[114]

Photoacoustic imaging is a potential technique for non-invasive tissue imaging, but improved photoacoustic contrast agents are still required.[115] Crudden synthesized carboxylic acid terminated benzimidazolium functionalized AuNPs that gave reproducible photoacoustic signals when irradiated with a pulsed laser.[97] A linear relationship was observed of the photoacoustic signal with respect to the NHC–AuNP concentration. While the possibility of using NHC–AuNPs as photoacoustic probes has been demonstrated, their use for *in vitro* tissue imaging has yet to be realized.

Conclusions and outlook

NHCs are reinvigorating the fields of gold surface chemistry and nanotechnology due to their tunability and stability. These advantages over thiols have made NHCs the next generation ligand choice for surface scientists. Tuning the wingtips leads to fundamental changes on the gold surface, including how NHCs bind and whether they are mobile. Tuning the backbone on the NHC allows for numerous applications *via* post-synthetic modification reactions. Notably, these post-synthetic reactions are only possible due to NHCs' incredible surface stability on gold. Their stability has been tested for pH swings, heating, oxidation, and even biological fluids, such as buffers or serums. Finally, NHCs have shown their versatility for applications ranging from biosensing, to surface patterning, to microelectronics.

We envision that gold's inertness combined with NHCs' high degree of tunability will lead to more applications that were previously challenging with thiol ligands. While initial studies have already been reported on biomedical applications, this area should expand substantially to take advantage of the improved biocompatibility due to NHCs' stability. Likewise, heterogenous catalysis could benefit from the longer lasting links of NHCs to gold nanoparticles. Finally, although research on NHC wingtips has proceeded with standard NHCs, there are still very few reports to date on non-standard NHCs on gold surfaces. Given the applications for non-standard NHCs in organometallic chemistry, this research direction could lead to fascinating new surface science on gold.

Conflicts of interest

There are no conflicts to declare.

Acknowledgements

This was supported by the National Science Foundation under grant numbers CHE-2108328 (G. K. and D. M. J.) and CHE-2108330 (R. L. T. and J. P. C.). Any opinions, findings, and conclusions or recommendations expressed in this material are those of the authors and do not necessarily reflect the views of the National Science Foundation.

References

1 D. A. Giljohann, D. S. Seferos, W. L. Daniel, M. D. Massich, P. C. Patel and C. A. Mirkin, *Angew. Chem., Int. Ed.*, 2010, **49**, 3280–3294.
2 E. Boisselier and D. Astruc, *Chem. Soc. Rev.*, 2009, **38**, 1759–1782.
3 G. Zhang, *Nanotechnol. Rev.*, 2013, **2**, 269–288.
4 K. Saha, S. S. Agasti, C. Kim, X. Li and V. M. Rotello, *Chem. Rev.*, 2012, **112**, 2739–2779.
5 S. Kang, S. E. Byeon and H. J. Yoon, *Bull. Korean Chem. Soc.*, 2021, **42**, 712–723.
6 L. Pasquato, P. Pengo and P. Scrimin, *J. Mater. Chem.*, 2004, **14**, 3481–3487.
7 R. Jin, C. Zeng, M. Zhou and Y. Chen, *Chem. Rev.*, 2016, **116**, 10346–10413.
8 C. Vericat, M. E. Vela, G. Benitez, P. Carro and R. C. Salvarezza, *Chem. Soc. Rev.*, 2010, **39**, 1805–1834.
9 J. J. Gooding and S. Ciampi, *Chem. Soc. Rev.*, 2011, **40**, 2704–2718.
10 M. H. Schoenfisch and J. E. Pemberton, *J. Am. Chem. Soc.*, 1998, **120**, 4502–4513.
11 T. M. Willey, A. L. Vance, T. van Buuren, C. Bostedt, L. J. Terminello and C. S. Fadley, *Surf. Sci.*, 2005, **576**, 188–196.
12 Y. Li, J. Huang, R. T. McIver Jr. and J. C. Hemminger, *J. Am. Chem. Soc.*, 1992, **114**, 2428–2432.
13 N. Garg, E. Carrasquillo-Molina and T. R. Lee, *Langmuir*, 2002, **18**, 2717–2726.
14 F. Li, H. Zhang, B. Dever, X.-F. Li and X. C. Le, *Bioconjugate Chem.*, 2013, **24**, 1790–1797.
15 E. Delamarche, B. Michel, H. Kang and C. Gerber, *Langmuir*, 1994, **10**, 4103–4108.
16 M. Borzenkov, G. Chirico, L. D'Alfonso, L. Sironi, M. Collini, E. Cabrini, G. Dacarro, C. Milanese, P. Pallavicini, A. Taglietti, C. Bernhard and F. Denat, *Langmuir*, 2015, **31**, 8081–8091.
17 J. Huang and J. C. Hemminger, *J. Am. Chem. Soc.*, 1993, **115**, 3342–3343.
18 D. A. Hutt and G. J. Leggett, *J. Phys. Chem.*, 1996, **100**, 6657–6662.
19 Y. Zhang, R. H. Terrill and P. W. Bohn, *Chem. Mater.*, 1999, **11**, 2191–2198.
20 N. T. Flynn, T. N. T. Tran, M. J. Cima and R. Langer, *Langmuir*, 2003, **19**, 10909–10915.
21 K. Jans, K. Bonroy, R. De Palma, G. Reekmans, H. Jans, W. Laureyn, M. Smet, G. Borghs and G. Maes, *Langmuir*, 2008, **24**, 3949–3954.

Open Access Article. Published on 07 November 2022. Downloaded on 11/7/2025 11:57:10 PM.
This article is licensed under a Creative Commons Attribution-NonCommercial 3.0 Unported Licence.

22 L. M. Demers, C. A. Mirkin, R. C. Mucic, R. A. Reynolds, R. L. Letsinger, R. Elghanian and G. Viswanadham, *Anal. Chem.*, 2000, **72**, 5535–5541.
23 M. Mora, M. C. Gimeno and R. Visbal, *Chem. Soc. Rev.*, 2019, **48**, 447–462.
24 S. P. Nolan, *Acc. Chem. Res.*, 2011, **44**, 91–100.
25 N. Marion and S. P. Nolan, *Chem. Soc. Rev.*, 2008, **37**, 1776–1782.
26 S. Gaillard, C. S. J. Cazin and S. P. Nolan, *Acc. Chem. Res.*, 2012, **45**, 778–787.
27 B. Dominelli, J. D. G. Correia and F. E. Kühn, *J. Organomet. Chem.*, 2018, **866**, 153–164.
28 M. Porchia, M. Pellei, M. Marinelli, F. Tisato, F. Del Bello and C. Santini, *Eur. J. Med. Chem.*, 2018, **146**, 709–746.
29 F. Guarra, A. Pratesi, C. Gabbiani and T. Biver, *J. Inorg. Biochem.*, 2021, **217**, 111355.
30 B. Bertrand and A. Casini, *Dalton Trans.*, 2014, **43**, 4209–4219.
31 A. Gómez-Suárez, D. J. Nelson, D. G. Thompson, D. B. Cordes, D. Graham, A. M. Z. Slawin and S. P. Nolan, *Beilstein J. Org. Chem.*, 2013, **9**, 2216–2223.
32 R. Visbal, I. Ospino, J. M. López-de-Luzuriaga, A. Laguna and M. C. Gimeno, *J. Am. Chem. Soc.*, 2013, **135**, 4712–4715.
33 R. Visbal, J. M. López-de-Luzuriaga, A. Laguna and M. C. Gimeno, *Dalton Trans.*, 2014, **43**, 328–334.
34 E. C. Hurst, K. Wilson, I. J. S. Fairlamb and V. Chechik, *New J. Chem.*, 2009, **33**, 1837–1840.
35 J. Vignolle and T. D. Tilley, *Chem. Commun.*, 2009, 7230–7232, DOI: 10.1039/B913884F.
36 T. Weidner, J. E. Baio, A. Mundstock, C. Große, S. Karthäuser, C. Bruhn and U. Siemeling, *Aust. J. Chem.*, 2011, **64**, 1177–1179.
37 A. V. Zhukhovitskiy, M. G. Mavros, T. Van Voorhis and J. A. Johnson, *J. Am. Chem. Soc.*, 2013, **135**, 7418–7421.
38 C. M. Crudden, J. H. Horton, I. I. Ebralidze, O. V. Zenkina, A. B. McLean, B. Drevniok, Z. She, H.-B. Kraatz, N. J. Mosey, T. Seki, E. C. Keske, J. D. Leake, A. Rousina-Webb and G. Wu, *Nat. Chem.*, 2014, **6**, 409–414.
39 C. Eisen, J. M. Chin and M. R. Reithofer, *Chem. – Asian J.*, 2021, **16**, 3026–3037.
40 M. Koy, P. Bellotti, M. Das and F. Glorius, *Nat. Catal.*, 2021, **4**, 352–363.
41 S. R. Thomas and A. Casini, *J. Organomet. Chem.*, 2021, **938**, 121743.
42 S. Engel, E.-C. Fritz and B. J. Ravoo, *Chem. Soc. Rev.*, 2017, **46**, 2057–2075.
43 H. Shen, G. Tian, Z. Xu, L. Wang, Q. Wu, Y. Zhang, B. K. Teo and N. Zheng, *Coord. Chem. Rev.*, 2022, **458**, 214425.
44 C. A. Smith, M. R. Narouz, P. A. Lummis, I. Singh, A. Nazemi, C.-H. Li and C. M. Crudden, *Chem. Rev.*, 2019, **119**, 4986–5056.
45 P. Bellotti, M. Koy, M. N. Hopkinson and F. Glorius, *Nat. Rev. Chem.*, 2021, **5**, 711–725.
46 C. R. Larrea, C. J. Baddeley, M. R. Narouz, N. J. Mosey, J. H. Horton and C. M. Crudden, *ChemPhysChem*, 2017, **18**, 3536–3539.
47 M. Jain, U. Gerstmann, W. G. Schmidt and H. Aldahhak, *J. Comput. Chem.*, 2022, **43**, 413–420.
48 L. M. Sherman, S. L. Strausser, R. K. Borsari, D. M. Jenkins and J. P. Camden, *Langmuir*, 2021, **37**, 5864–5871.
49 M. J. Trujillo, S. L. Strausser, J. C. Becca, J. F. DeJesus, L. Jensen, D. M. Jenkins and J. P. Camden, *J. Phys. Chem. Lett.*, 2018, **9**, 6779–6785.
50 A. Bakker, A. Timmer, E. Kolodzeiski, M. Freitag, H. Y. Gao, H. Mönig, S. Amirjalayer, F. Glorius and H. Fuchs, *J. Am. Chem. Soc.*, 2018, **140**, 11889–11892.
51 J. Ren, M. Freitag, Y. Gao, P. Bellotti, M. Das, B. Schulze Lammers, H. Mönig, Y. Zhang, C. G. Daniliuc, S. Du, H. Fuchs and F. Glorius, *Angew. Chem., Int. Ed.*, 2022, **61**, e202115104.
52 A. Bakker, M. Freitag, E. Kolodzeiski, P. Bellotti, A. Timmer, J. Ren, B. Schulze Lammers, D. Moock, H. W. Roesky, H. Mönig, S. Amirjalayer, H. Fuchs and F. Glorius, *Angew. Chem., Int. Ed.*, 2020, **59**, 13643–13646.
53 M. N. Hopkinson, C. Richter, M. Schedler and F. Glorius, *Nature*, 2014, **510**, 485–496.
54 A. Inayeh, R. R. K. Groome, I. Singh, A. J. Veinot, F. C. de Lima, R. H. Miwa, C. M. Crudden and A. B. McLean, *Nat. Commun.*, 2021, **12**, 4034.
55 G. Lovat, E. A. Doud, D. Lu, G. Kladnik, M. S. Inkpen, M. L. Steigerwald, D. Cvetko, M. S. Hybertsen, A. Morgante, X. Roy and L. Venkataraman, *Chem. Sci.*, 2019, **10**, 930–935.
56 S. Dery, S. Kim, G. Tomaschun, D. Haddad, A. Cossaro, A. Verdini, L. Floreano, T. Klüner, F. D. Toste and E. Gross, *Chem. – Eur. J.*, 2019, **25**, 15067–15072.
57 S. Amirjalayer, A. Bakker, M. Freitag, F. Glorius and H. Fuchs, *Angew. Chem., Int. Ed.*, 2020, **59**, 21230–21235.
58 J. F. DeJesus, M. J. Trujillo, J. P. Camden and D. M. Jenkins, *J. Am. Chem. Soc.*, 2018, **140**, 1247–1250.
59 Z. Li, K. Munro, M. R. Narouz, A. Lau, H. Hao, C. M. Crudden and J. H. Horton, *ACS Appl. Mater. Interfaces*, 2018, **10**, 17560–17570.
60 S. Dery, S. Kim, G. Tomaschun, I. Berg, D. Feferman, A. Cossaro, A. Verdini, L. Floreano, T. Klüner, F. D. Toste and E. Gross, *J. Phys. Chem. Lett.*, 2019, **10**, 5099–5104.
61 E. Amit, L. Dery, S. Dery, S. Kim, A. Roy, Q. Hu, V. Gutkin, H. Eisenberg, T. Stein, D. Mandler, F. Dean Toste and E. Gross, *Nat. Commun.*, 2020, **11**, 5714.
62 C. M. Crudden, J. H. Horton, M. R. Narouz, Z. Li, C. A. Smith, K. Munro, C. J. Baddeley, C. R. Larrea, B. Drevniok, B. Thanabalasingam, A. B. McLean, O. V. Zenkina, I. I. Ebralidze, Z. She, H.-B. Kraatz, N. J. Mosey, L. N. Saunders and A. Yagi, *Nat. Commun.*, 2016, **7**, 12654.
63 G. Wang, A. Rühling, S. Amirjalayer, M. Knor, J. B. Ernst, C. Richter, H.-J. Gao, A. Timmer, H.-Y. Gao, N. L. Doltsinis, F. Glorius and H. Fuchs, *Nat. Chem.*, 2017, **9**, 152–156.
64 L. Jiang, B. Zhang, G. Médard, A. P. Seitsonen, F. Haag, F. Allegretti, J. Reichert, B. Kuster, J. V. Barth and A. C. Papageorgiou, *Chem. Sci.*, 2017, **8**, 8301–8308.
65 D. T. Nguyen, M. Freitag, M. Körsgen, S. Lamping, A. Rühling, A. H. Schäfer, M. H. Siekman, H. F. Arlinghaus, W. G. van der Wiel, F. Glorius and B. J. Ravoo, *Angew. Chem., Int. Ed.*, 2018, **57**, 11465–11469.
66 J. Ren, M. Freitag, C. Schwermann, A. Bakker, S. Amirjalayer, A. Rühling, H.-Y. Gao, N. L. Doltsinis, F. Glorius and H. Fuchs, *Nano Lett.*, 2020, **20**, 5922–5928.
67 J. F. DeJesus, L. M. Sherman, D. J. Yohannan, J. C. Becca, S. L. Strausser, L. F. P. Karger, L. Jensen, D. M. Jenkins and J. P. Camden, *Angew. Chem., Int. Ed.*, 2020, **59**, 7585–7590.
68 S. Qi, Q. Ma, X. He and Y. Tang, *Colloids Surf., A*, 2018, **538**, 488–493.
69 A. Krzykawska, M. Wróbel, K. Kozieł and P. Cyganik, *ACS Nano*, 2020, **14**, 6043–6057.
70 V. R. Samuel and K. J. Rao, *Biosens. Bioelectron.: X*, 2022, **11**, 100216.
71 B. G. Andryukov, N. N. Besednova, R. V. Romashko, T. S. Zaporozhets and T. A. Efimov, *Biosensors*, 2020, **10**, 11.
72 B. E. Rapp, F. J. Gruhl and K. Länge, *Anal. Bioanal. Chem.*, 2010, **398**, 2403–2412.
73 Z. Li, K. Munro, I. I. Ebralize, M. R. Narouz, J. D. Padmos, H. Hao, C. M. Crudden and J. H. Horton, *Langmuir*, 2017, **33**, 13936–13944.
74 Z. Li, M. R. Narouz, K. Munro, B. Hao, C. M. Crudden, J. H. Horton and H. Hao, *ACS Appl. Mater. Interfaces*, 2017, **9**, 39223–39234.
75 J. Heo and S. Z. Hua, *Sensors*, 2009, **9**, 4483–4502.
76 R. M. Mayall, C. A. Smith, A. S. Hyla, D. S. Lee, C. M. Crudden and V. I. Birss, *ACS Sens.*, 2020, **5**, 2747–2752.
77 I. Singh, D. S. Lee, S. Huang, H. Bhattacharjee, W. Xu, J. F. McLeod, C. M. Crudden and Z. She, *Chem. Commun.*, 2021, **57**, 8421–8424.
78 F. von Wrochem, D. Gao, F. Scholz, H.-G. Nothofer, G. Nelles and J. M. Wessels, *Nat. Nanotechnol.*, 2010, **5**, 618–624.
79 A. Lv, M. Freitag, K. M. Chepiga, A. H. Schäfer, F. Glorius and L. Chi, *Angew. Chem., Int. Ed.*, 2018, **57**, 4792–4796.
80 Z. She, M. R. Narouz, C. A. Smith, A. MacLean, H.-P. Loock, H.-B. Kraatz and C. M. Crudden, *Chem. Commun.*, 2020, **56**, 1275–1278.
81 E. A. Doud, M. S. Inkpen, G. Lovat, E. Montes, D. W. Paley, M. L. Steigerwald, H. Vázquez, L. Venkataraman and X. Roy, *J. Am. Chem. Soc.*, 2018, **140**, 8944–8949.
82 Z. Wang, M. Das, C. Gutheil, H. Osthues, F. Strieth-Kalthoff, A. Timmer, N. L. Doltsinis, W. Wang, L. Chi and F. Glorius, *J. Mater. Chem. C*, 2022, **10**, 8589–8595.
83 D. T. Nguyen, M. Freitag, C. Gutheil, K. Sotthewes, B. J. Tyler, M. Böckmann, M. Das, F. Schlüter, N. L. Doltsinis, H. F. Arlinghaus, B. J. Ravoo and F. Glorius, *Angew. Chem., Int. Ed.*, 2020, **59**, 13651–13656.
84 X. Hu, Y. Zhang, T. Ding, J. Liu and H. Zhao, *Front. Bioeng. Biotechnol.*, 2020, **8**, 990.

 This journal is © The Royal Society of Chemistry 2022

Open Access Article. Published on 07 November 2022. Downloaded on 11/7/2025 11:57:10 PM.
This article is licensed under a Creative Commons Attribution-NonCommercial 3.0 Unported Licence.

85 E. C. Dreaden, A. M. Alkilany, X. Huang, C. J. Murphy and M. A. El-Sayed, *Chem. Soc. Rev.*, 2012, **41**, 2740–2779.
86 F. Y. Kong, J. W. Zhang, R. F. Li, Z. X. Wang, W. J. Wang and W. Wang, *Molecules*, 2017, 22.
87 M. J. MacLeod, A. J. Goodman, H. Z. Ye, H. V. Nguyen, T. Van Voorhis and J. A. Johnson, *Nat. Chem.*, 2019, **11**, 57–63.
88 M. Bélanger-Bouliga, R. Mahious, P. I. Pitroipa and A. Nazemi, *Dalton Trans.*, 2021, **50**, 5598–5606.
89 K. Salorinne, R. W. Y. Man, C.-H. Li, M. Taki, M. Nambo and C. M. Crudden, *Angew. Chem., Int. Ed.*, 2017, **56**, 6198–6202.
90 A. J. Young, M. Sauer, G. M. D. M. Rubio, A. Sato, A. Foelske, C. J. Serpell, J. M. Chin and M. R. Reithofer, *Nanoscale*, 2019, **11**, 8327–8333.
91 R. Ye, A. V. Zhukhovitskiy, R. V. Kazantsev, S. C. Fakra, B. B. Wickemeyer, F. D. Toste and G. A. Somorjai, *J. Am. Chem. Soc.*, 2018, **140**, 4144–4149.
92 A. J. Young, C. J. Serpell, J. M. Chin and M. R. Reithofer, *Chem. Commun.*, 2017, **53**, 12426–12429.
93 R. W. Y. Man, C.-H. Li, M. W. A. MacLean, O. V. Zenkina, M. T. Zamora, L. N. Saunders, A. Rousina-Webb, M. Nambo and C. M. Crudden, *J. Am. Chem. Soc.*, 2018, **140**, 1576–1579.
94 N. A. Nosratabad, Z. Jin, L. Du, M. Thakur and H. Mattoussi, *Chem. Mater.*, 2021, **33**, 921–933.
95 L. Zhang, Z. Wei, S. Thanneeru, M. Meng, M. Kruzyk, G. Ung, B. Liu and J. He, *Angew. Chem., Int. Ed.*, 2019, **58**, 15834–15840.
96 N. Sun, S. T. Zhang, F. Simon, A. M. Steiner, J. Schubert, Y. Du, Z. Qiao, A. Fery and F. Lissel, *Angew. Chem., Int. Ed.*, 2021, **60**, 3912–3917.
97 K. Salorinne, R. W. Y. Man, C. H. Li, M. Taki, M. Nambo and C. M. Crudden, *Angew. Chem., Int. Ed.*, 2017, **56**, 6198–6202.
98 A. J. Young, C. Eisen, G. M. D. M. Rubio, J. M. Chin and M. R. Reithofer, *J. Inorg. Biochem.*, 2019, **199**, 110707.
99 D. T. H. Nguyen, M. Bélanger-Bouliga, L. R. Shultz, A. Maity, T. Jurca and A. Nazemi, *Chem. Mater.*, 2021, **33**, 9588–9600.
100 M. J. MacLeod and J. A. Johnson, *J. Am. Chem. Soc.*, 2015, **137**, 7974–7977.
101 S. R. Thomas, W. Yang, D. J. Morgan, T. E. Davies, J. J. Li, R. A. Fischer, J. Huang, N. Dimitratos and A. Casini, *Chem. – Eur. J.*, 2022, e202201575.
102 L. M. Sherman, M. D. Finley, R. K. Borsari, N. Schuster-Little, S. L. Strausser, R. J. Whelan, D. M. Jenkins and J. P. Camden, *ACS Omega*, 2022, **7**, 1444–1451.
103 M. R. Narouz, C.-H. Li, A. Nazemi and C. M. Crudden, *Langmuir*, 2017, **33**, 14211–14219.
104 V. Ramalingam, *Adv. Colloid Interface Sci.*, 2019, **271**, 101989.
105 O. V. Kuznetsova, G. M. D. M. Rubio, B. K. Keppler, J. M. Chin, M. R. Reithofer and A. R. Timerbaev, *Anal. Biochem.*, 2020, **611**, 114003.
106 N. Bridonneau, L. Hippolyte, D. Mercier, D. Portehault, M. Desage-El Murr, P. Marcus, L. Fensterbank, C. Chanéac and F. Ribot, *Dalton Trans.*, 2018, **47**, 6850–6859.
107 J. Crespo, Y. Guari, A. Ibarra, J. Larionova, T. Lasanta, D. Laurencin, J. M. López-de-Luzuriaga, M. Monge, M. E. Olmos and S. Richeter, *Dalton Trans.*, 2014, **43**, 15713–15718.
108 N. L. Dominique, S. L. Strausser, J. E. Olson, W. C. Boggess, D. M. Jenkins and J. P. Camden, *Anal. Chem.*, 2021, **93**, 13534–13538.
109 T. Ishida, T. Murayama, A. Taketoshi and M. Haruta, *Chem. Rev.*, 2020, **120**, 464–525.
110 D. Ventura-Espinosa, S. Martín and J. A. Mata, *J. Catal.*, 2019, **375**, 419–426.
111 D. Ventura-Espinosa, S. Martín, H. García and J. A. Mata, *J. Catal.*, 2021, **394**, 113–120.
112 X.-X. Gou, T. Liu, Y.-Y. Wang and Y.-F. Han, *Angew. Chem., Int. Ed.*, 2020, **59**, 16683–16689.
113 C. M. Pitsillides, E. K. Joe, X. Wei, R. R. Anderson and C. P. Lin, *Biophys. J.*, 2003, **84**, 4023–4032.
114 M. A. Mackey, M. R. K. Ali, L. A. Austin, R. D. Near and M. A. El-Sayed, *J. Phys. Chem. B*, 2014, **118**, 1319–1326.
115 L. Nie and X. Chen, *Chem. Soc. Rev.*, 2014, **43**, 7132–7170.